# AN EXPERIMENTAL STUDY FOR A MINIATURE
## STIRLING REFRIGERATOR

Shimo Li   and   Chen Guobang
Zhixiu Huang   Fagao Zhang

Cryogenic Engineering Laboratory
Zhejiang University, China

Cuangji Cui and Jiazhang Li

Low Temperature Physics Laboratory
Beijing University, China

In this paper, experimental results of a miniature two-stage
Stirling cryocooler are introduced. The influence of filling gas
pressure and refrigeration temperature on the refrigerating capacity
along with the relationship between parameters has been measured. The
valley pressure corresponding to the lowest refrigeration temperature
and the cooldown time versus operating pressure have been discussed.
The coefficient of performance and thermodynamic efficiency of the
cryocooler have been calculated based on experimental data.

Key words: Cryocooler; cryogenics for infra-red detectors; miniature
Stirling refrigerators; refrigeration.

## 1.   Introduction

In recent years, we have studied the thermodynamic characteristics of both types 3Ly-03/194
which is a small single stage refrigerator [1] and A3040 Stirling cycle refrigerator which is a
miniature two-stage refrigerator. Measurements have been made of refrigeration temperature,
operation pressure, cooling capacity, cooldown time along with the relationship between them. In
addition, the influence of surrounding conditions and contamination of the regenerator on the
performance of the refrigerator is also considered. In the following, the experimental study on
the miniature two-stage Stirling refrigerator will be discussed.

## 2.   Structural Features of the Cryocooler

This miniature two-stage Stirling refrigerator was built in Beijing University in 1972. Its
major specifications are listed in Table 1. The device was designed for refrigerating infra-red
detectors requiring a refrigeration temperature of about 25-30 K [2]. Most components of the
refrigerator are made of stainless steel. The cylinder and displacer define two low temperature
expansion spaces. There are two co-axially located regenerators in the displacer. Stacks of
stainless steel screen are used as regenerative packing material. A copper shield is installed on
the first cold head and there are several layers of Al-coated Mylar outside the shield to reduce
radiation loss. During the experiment the insulation space is about $5 \times 10^{-4}$ mmHg dynamic vacuum.
The second stage cold head and the cylinder made of oxygen-free copper, are connected together for
better thermal stability. The machine was operated at 1400 rpm. Helium gas is used for working
medium. The compressive heat of helium gas is carried away by cooling water.

## Table 1. Major specifications of A3040 Refrigerator

| Component | Unit | Value |
|---|---|---|
| Compressor-cylinder diameter/stroke/volume | $mm/mm/cm^3$ | 60/15/42.4 |
| Primary cylinder diameter/stroke/volume | $mm/mm/cm^3$ | 23.9/13/3.53 |
| Secondary cylinder diameter/stroke/volume | $mm/mm/cm^3$ | 15/13/2.3 |
| Length/diameter of the primary regenerator | mm/mm | 40/19 |
| Length/diameter of the secondary regenerator | mm/mm | 26/14.3 |
| Structure angle $\beta$ | degree | 60 |
| Volumetric phase angle $\phi$ | degree | 67 |
| Pressure phase angle $\theta$ | degree | 38 |
| Pressure parameter $\delta$ | dimensionless | 0.45 |
| Pressure ratio $\sigma$ | dimensionless | 2.67 |
| Filling gas pressure | bar | 6.5 |
| 1st and 2nd stage temperature $T_m/T_e$ | K/K | 95/30 |
| 1st and 2nd stage regenerators packing material | mesh | 250/300 |
| 1st and 2nd theoretical refrigerating capacity $Q_m/Q_e$ | watts/watts | 39.4/25.7 |
| Weight of the refrigerator (exclude the motor) | Kg | 17 |

For refrigeration power measurement, 6 m of 0.2 mm constantan wire is coiled on the copper cylinder of the secondary cold head. The electric resistance of the wire is about 50 ohm at room temperature. Power is supplied by an adjustable D.C. supply. The heating power is less than 12 W.

Temperature is measured at three points: $T_e$ is measured with a Ni-Cr-Au-Fe thermocouple at the secondary cold head, while $T_m$ and $T_o$ are measured with Cu-constantan thermocouples at the hot ends of the secondary and the primary cylinder, respectively, (see Fig. 1).
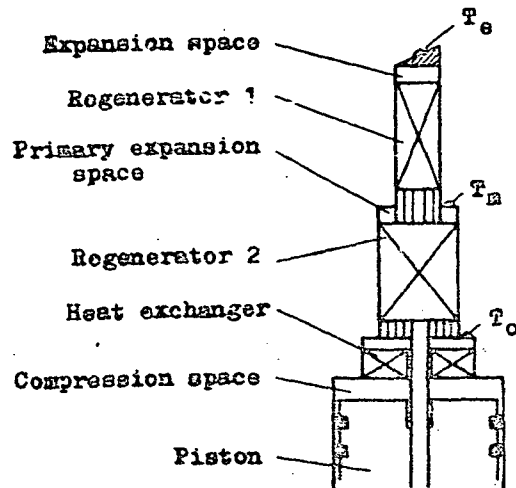
Figure 1. Arrangement for temperature measurement.

Type UJ-26 electric potential meters (with a precision of 0.1 µV) and PZ26b direct digital voltage meters are used in measuring. Good thermal contact of the thermometer with cold head is provided.

## 3. Experimental Results

The relationship of the lowest refrigeration temperature, cooldown time and filling gas pressure have been measured. The experiment was made under bad conditions, e. g. the outdoor temperature was about $35^\circ C$. The temperature of the cooling water was $30^\circ C$, and the room temperature was not lower than $30^\circ C$.

### 3.1 The Lowest Refrigeration Temperature

Under a condition of no heat load, a minimum is found in the lowest refrigeration temperature as a function of filling pressure. The relationship between them is shown in figure 2. The refrigeration temperature will increase when the pressure is either higher or lower than the optimum pressure (in the measurement on 3LV-08/194 refrigerator, two optimum pressures have been observed [1]).

### 3.2 Cooldown Time

The time required for the temperatures $T_m$ and $T_e$ of first and second stage cold heads to decrease from room temperature to the lowest equilibrium temperature under a given operating pressure is called the cooldown time. Figure 3 shows these temperature-time curves under a filling gas pressure of 7.5 bar. It seems that the cooldown time of the machine on the order of 15 minutes is somewhat longer than that of a normal one under normal operating pressure. Probably this is because of the larger heat capacity of the secondary cold head and the copper block of the 2nd cylinder. The cooling curve takes a similar shape with that of reference [3]. As filling gas pressure increases the unloaded cooldown time is shortened (see Fig. 4). When the filling gas pressure decreases from 7.5 bar to 3.5 bar, the cooldown time almost doubles (from 15 minutes to 34 minutes).
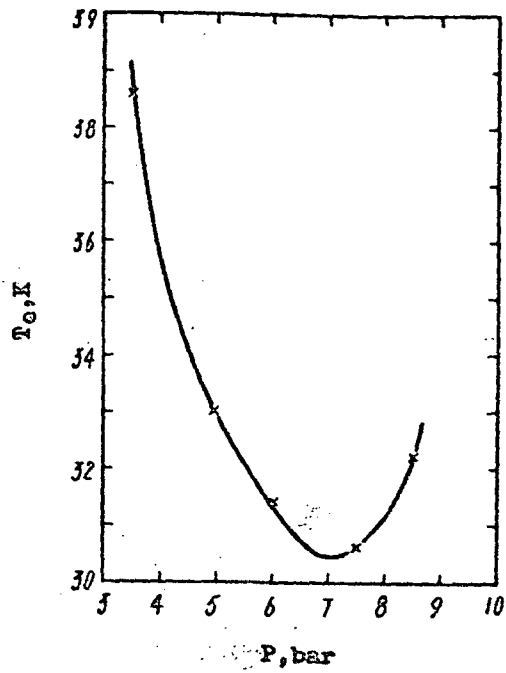
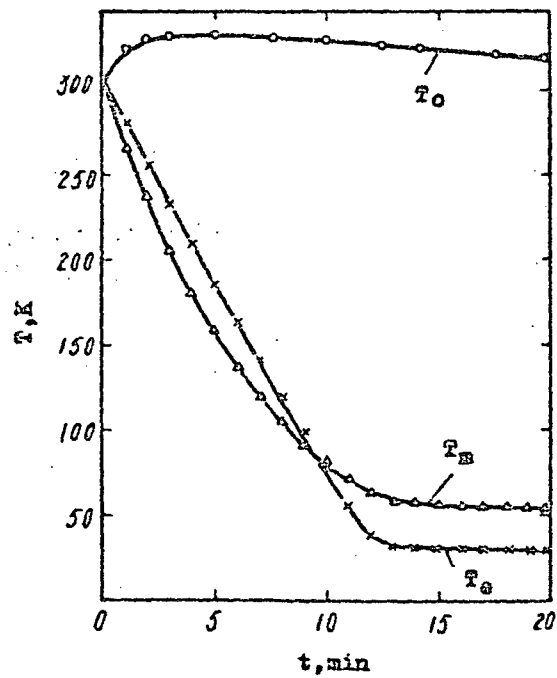Figure 2. Lowest refrigeration temperature versus operation pressure.



Figure 3. Cooldown curve of miniature two-stage Stirling refrigerator.

Experimental results show that the cooling curves of $T_e$ and $T_m$ are similar to each other. The temperature of the hot end of the 1st cylinder quickly reached a steady state. At the initial stage, the decreasing rate of $T_m$ is greater than that of $T_e$. Then two cooling curves of $T_m$ and $T_e$ intersect each other. At last, $T_m$ and $T_e$ curves almost reach their equilibrium temperature simultaneously.

### 3.3 Cooling Capacity

The refrigeration temperature $T_e$ varies approximately linearly with cooling capacity $Q_e$ when the filling pressure is under 9 bar (see Fig. 5). At a given refrigeration temperature $T_e$, the cooling capacity $Q_e$ increases at the pressure increases. The critical heating power under which the machine is at the full-loaded state is about 9.5 - 10 W when filling gas pressures are 6.5 bar and 7.5 bar (see Fig. 5). While the heating power is increased continually temperatures of the 1st and 2nd stage are reversed, i.e., $T_m < T_e$. Since only a few watts and a temperature just below 40 K are required for practical applications, the cooling capacity required cannot be supercritical. Figure 5 also shows that the variation extent of $T_m$ versus cooling capacity is not great. While the 2nd stage cooling capacity is increased from zero to the critical value, the corresponding difference of the 1st stage temperature is approximately 10 K.
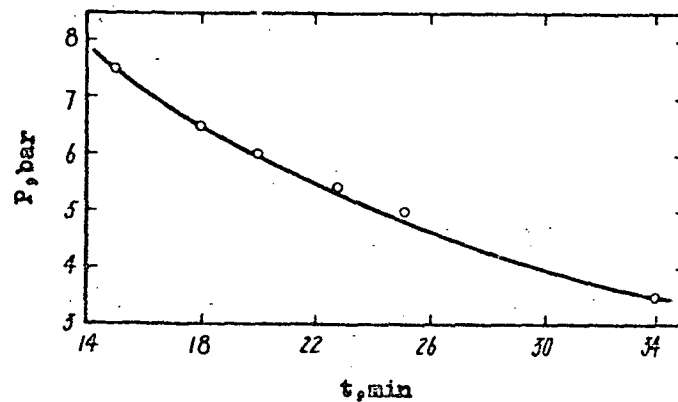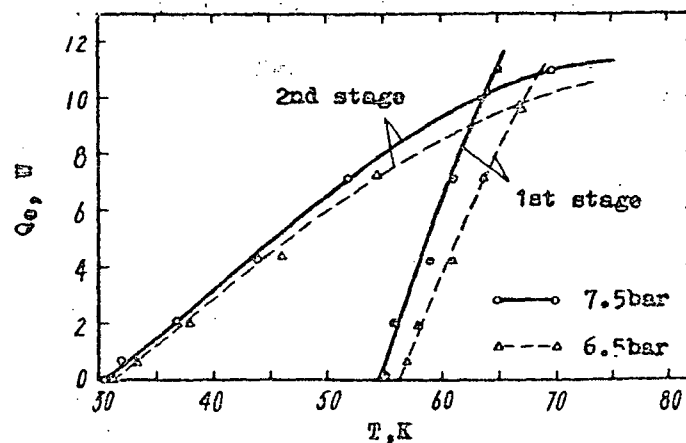


Figure 4. Filling gas pressure versus cooldown time.



Figure 5. Cooling capacity versus refrigeration temperature.

75

### 3.4 Thermodynamic Efficiency

Coefficient of performance $\epsilon$ and thermodynamic efficiency $\eta_c$ are defined as follows

$$\epsilon = Q_e/N \tag{1}$$

$$\eta_c = \epsilon/\epsilon_i = \epsilon \, \frac{T_o - T_e}{T_e} \tag{2}$$

where  $Q_e$ = actual cooling capacity, W
$N$ = actual input power, W
$\epsilon_i$ = coefficient of performance for Carnot cycle
$T_o$ = ambient temperature, K

According to thermodynamic principle, the input power increases while the temperature $T_e$ of the expansion space decreases due to the reduction in heat displacement of unit working medium. Thus both of the coefficient of performance and thermodynamic efficiency will be reduced. Figure 6 shows results calculated from experimental data.

Figure 6 shows an optimize-region for the cycle efficiency of the refrigerator correlated to the thermodynamic efficiency $\eta_c$ of the Carnot cycle, i.e. the efficiency of the machine is highest when operating at corresponding temperatures in this region. However, the coefficient, $\epsilon$, which depends only upon the temperature ratio, increases almost linearly with the refrigeration temperature. On the other hand, it is also learned from studying the effect of dead expansion space $S_{ed}$ on $\eta_c$ and $\epsilon$, that a temperature increase and a reduction in efficiency $\eta_c$ take place as $S_{ed}$ increases while $\epsilon$ continues to increase. In fact, this shows that it is unreasonable to evaluate cycle efficiency at different refrigeration temperature by using $\epsilon$ only.
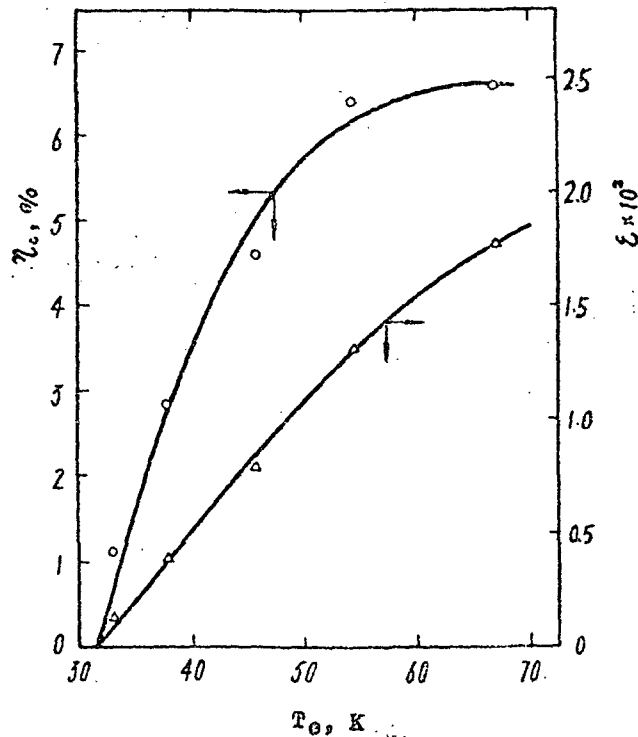


Figure 6.  Variation of coefficient $\epsilon$ and thermodynamic efficiency $\eta_c$ with refrigeration temperature $T_e$.
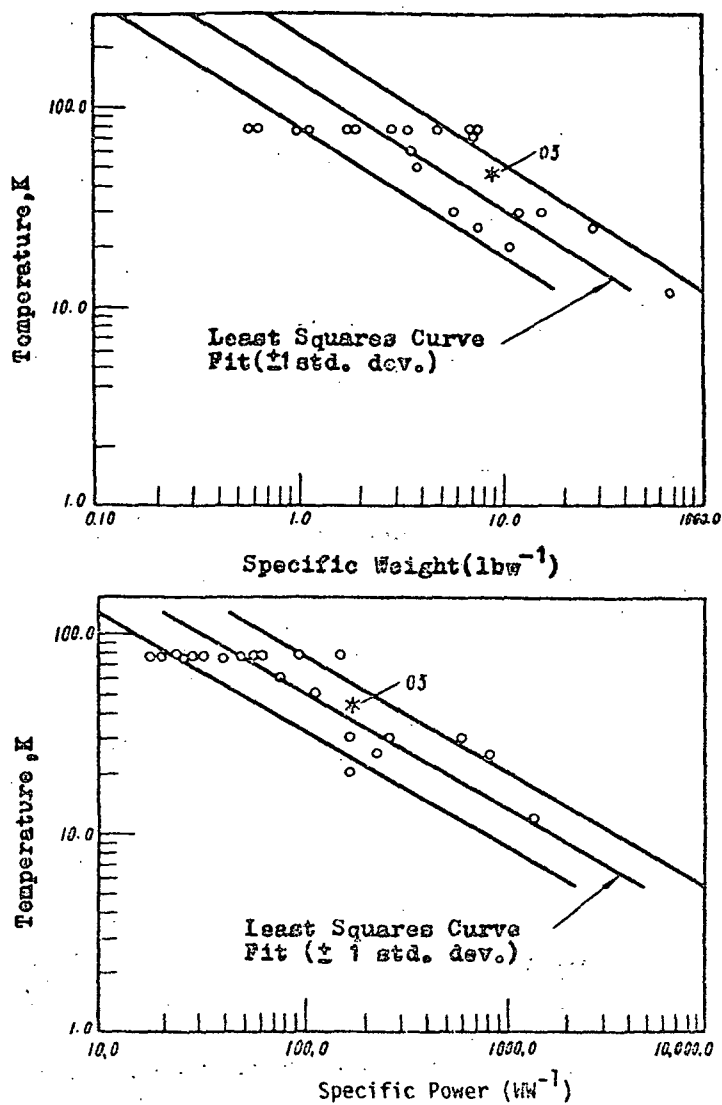
Figure 7. Characteristics of miniature Stirling refrigerator.

Figure 7 shows power and weight characteristics of Stirling refrigerators [4]. Calculated data of our experimental machine are also plotted in the figure (plotted by "*" and numbered 03). From figure 7 it can be seen that specific weight and specific power of our cryocooler are in the middle of the wide band.

## 4. Discussion

Using experimental data of temperatures and refrigeration powers measured, the different cold losses of the refrigerator are evaluated according to reference [5]. Calculated net cooling capacities are essentially consistent with measured ones. Now the discussion will be made in the following two problems.

### 4.1 An Optimum Pressure in Figure 2.

A number of experiments on two refrigerators proved that the working pressure has a strong effect on refrigeration temperature and that there is an optimum pressure on pressure versus refrigeration temperature diagram (Fig. 2). It could be explained as follows.

77

Major cold losses of a refrigerator include shuttle loss, pumping loss, heat conduction loss of the displacer and the cylinder wall, and regenerator inefficiency loss, etc. There are over 30 parameters in all equations which are applied to calculate cold losses. Most of those parameters are structure ones, and only one fourth of those are physical parameters of working medium and operation parameters. Under our operating condition of the machine, the specific heat and thermal conductivity of the working medium undergoes a small change when the pressure changes. The shuttle loss and heat conduction loss are mainly functions of the temperature gradient in the axis direction, but independent of working pressure [6]. The operating temperature of this machine is far away from the critical temperature of the working medium He, so that the enthalpy flow loss caused by the nonideal property of the working as is negligible. Thus the major cold losses which have apparent relations with the pressure are the following three terms:

Pumping loss

$$Q_{pu} = \frac{2(\pi D_c)^{0.6} L_{cy}(P_{max}-P_{min})^{1.6} c_p^{1.6}(T_w-T_e)S^{2.6}}{1.52 R^{1.6} K_g^{1.6}(\frac{T_w+T_e}{2})^{1.6}}$$

$$\doteq A (P_{max}-P_{min})^{1.6}$$

(3)

Friction heat loss in regenerator

$$Q_{rf} = \frac{(P_{max}+P_{min})^3 V_{cm}^3 f L_r}{2(ZRT_e)^3 g_c A_{reg}^2 \rho^2 D_e J}$$

$$\doteq B (P_{max}+P_{min})^3$$

(4)

Heat load due to limiting value of film coefficient in regenerator

$$Q_{rh} = (1-\eta_r) c_p(T_w-T_e) \frac{(P_{max}+P_{min}) V_{cm} N}{2RT_e Z}$$

$$\doteq C (P_{max}+P_{min})$$

(5)

The total pressure dependent loss is

$$Q_t \doteq A(P_{max}-P_{min})^{1.6} + B(P_{max}+P_{min})^3 + C(P_{max}+P_{min})$$

(6)

Experimental results and theoretical calculations show [5-7] that these terms account for a major portion of the total loss (over 60% normally) and affect cooling capacity or temperature significantly.

On the other hand the theoretical cooling capacity is proportional to the average operating pressure $P = \sqrt{Pmax \cdot Pmin}$ to the first approximation, i.e., it is a linear function of the pressure. But it is known from eq. (6) that the changing rate of the cold loss $Q_t$ increases with the pressure. Therefore, if the changing rate of the cold loss versus pressure is lower than that of theoretical cooling capacity, the net cooling capacity would have increased with pressure, i.e. the limiting refrigeration temperature of the machine could have decreased with pressure. On the contrary, the net cooling capacity should decrease while the pressure increases, i.e. the limiting refrigeration temperature will increase with the pressure. So there must exist an optimum pressure for the refrigerator. Reference [7] discussed the influence of the working pressure of refrigerators on the cooling capacity. As for the case when a possible low refrigeration temperature is required in small power consumption refrigeration, the machine has better operation near the optimum pressure. The advantage of low pressure operation is particularly apparent when the increment in pressure causes a rapid increase in regenerative heat loss.

78

Incidentally, if the working medium is $H_2$ instead of He, the corresponding highest pressure Pmax reaches the critical pressure of $H_2$ when filling gas pressure is greater than 4.5 bar. The lowest refrigeration temperature of the refrigerator cannot be lower than the critical temperature (33 K) of $H_2$ even though the pressure is increased continuously. Mean while the enthalpy flow loss reaches a considerable large value due to non-ideal property of the working medium.

## 4.2 Comment

Most of the structure parameters and operation conditions of the refrigerator, such as the gas distribution proportion in the 1st and 2nd stage cold chambers (20% and 80%, respectively) and the relative volume of dead spaces of the 1st and 2nd stage cold chambers corresponding to the largest displacement volume etc. are approaching normal values of practical refrigerators. But why is the refrigeration temperature still higher? First, the length and construction of the secondary regenerator is imperfect, e.g. the dead space of the regenerator is less than 1.5 times the largest volume of the cold space (normal values are 1.5 - 3.5 times). Second, the copper cylinder connected with the cold head of 2nd stage is so close to the 1st stage cold head (about 15 mm) that temperature distribution is unreasonable. The temperature difference $\Delta T = T_m - T_e$ is relatively small. Thirdly, the specific heat of the stainless steel packing material in the secondary regenerator will rapidly decrease and working medium He will increase, when the temperature is further reduced. This phenomenon leads to "thermal saturation" in a regenerator and reduces its efficiency. Besides, the experimental conditions were rather difficult, the temperature of the cooling water which was put into the compressor was too high, and therefore the hot end temperature of the primary regenerator was even higher than $40^{\circ}C$. Therefore, the structure of the 2nd stage regenerator has to be improved and the packing material has to be changed as well.

## 5. References

[1] Li, S. M., et al. Single Stirling Cycle Refrigerator, to be published. (1984).

[2] Cui, G. J., et al. Development Introduction of A3040 Miniature Stirling Refrigerator, (1972).

[3] Daniels, A. and du Pre, F. K., Advances in Cryogenic Engineering 16, 178-184, (1971).

[4] Wolfe, W. L. and Zissis, G. J.; The Infrared Handbook, Office of Naval Research, Department of the Navy, Arlington, VA, 15-31, (1978).

[5] AD-A 027055 (1976).

[6] Radebaugh, R., XV International Congress of Refrigeration, A1/2-16, Venice, Italy, (September, 1979).

[7] Walker, G., Cryocoolers, Plenum, (1983).